Study on crab-cavity-based longitudinal injection scheme and prototype realization of C-band crab cavity for electron storage rings

Guan-Hua Wang[1,2], Bo-Cheng Jiang[3], Jian-Hao Tan[4,*], Qing-Lei Zhang[4], Wen-Cheng Fang[4], Chang-Liang Li[4], Kun Wang[4], Xiao-Xia Huang[4], Sheng-Li Pu[1]

[1] *University of Shanghai for Science and Technology, Shanghai 200093, China*

[2] *Shanghai Institute of Applied Physics, Chinese Academy of Sciences, Shanghai 201800, China*

[3] *Laboratory for Ultrafast Transient Facility, Chongqing University, Chongqing 401331, China*

[4] *Shanghai Advanced Research Institute, Chinese Academy of Sciences, Shanghai 201204, China*

Abstract

A diffraction-limited storage ring with a multi-bend achromat lattice suffers from a small dynamic aperture for conventional off-axis injection. Thus, a longitudinal on-axis injection scheme based on a new type of crab cavity is proposed in this paper. Particle tracking simulations were performed to study the disturbance of the stored beam and the motion of the injected beam during the injection process. The possibility of multi-bunch injections was discussed. In addition, the effect of the long-range wake field induced by the stored beam was analyzed. A C-band standing-wave crab cavity was designed and produced as requested, and its field distribution was measured. The corresponding results are consistent with the simulation results.

Keywords: On-axis injection; Crab cavity; Bump orbit; Wakefield

1. Introduction

The fourth generation of synchrotron light sources have been developed. Accordingly, the natural emittance of the storage ring is reduced to several hundred pm-rad or less, which is close to the X-ray diffraction limit. This is mainly because of the application of the multibend achromat lattice. The emittance is inversely proportional to the cubic power of the number of dipole magnets [1,2,3]. Thus, increasing the number of dipoles is an effective way to reduce the emittance. The number of dipole magnets was found to increase such that the bending angle of each dipole magnet was smaller than the bending angle in the double- or triple-bend achromat lattice. The magnetic field of the quadrupoles should be stronger to suppress the dispersion caused by the dipoles. However, the strong quadrupole creates large negative chromaticities, which lead to head–tail instability and large tune shifts of off-momentum particles. Therefore, the magnetic field of the sextuple should be sufficiently strong to correct chromaticities slightly above zero. The nonlinear term increases as the sextupole magnetic field increases, reducing the dynamic aperture and leading to severe difficulties in injection [4,5]. The conventional 4-kicker bump injection scheme and its variants still demonstrate application potential owing to the actual situation of the storage rings, for example, ESRF-EBS [6], Spring8-II [7], and SLS-2 [8]. Therefore, development of a new injection scheme is important for general diffraction-limited storage rings. Several schemes have been proposed for addressing this issue. For example, (1) swap-out injection [9], (2) multiple kicker injection scheme [10], (3) longitudinal on-axis injection using a short-pulse kicker [11], and (4) on-axis injection scheme using a double-frequency or multi-frequency RF system [5,12,13,14].

Swapout injection has been adopted in many light sources under construction, such as APS-U, ALS-U, and HEPS [15,16]. Short-pulse kickers are incorporated to replace a stored bunch or bunch train with the least bunch current using a fresh bunch or bunch train. Thus, the requirement for a dynamic aperture was relaxed. An “accumulator ring” is used in some swap-out schemes to provide storage ring bunches and recycle the swapped-out bunches. However, storing a highly charged bunch is challenging because of single-bunch instability. Further, the accumulator ring adds considerable cost. For a swap-out without an accumulator ring, the swapped-out bunches are dumped into the swap-out dump. This may cause an increase in the radiation dose. The high-energy photon source (HEPS) adopted a compromise scheme in which the booster was used as the accumulator ring [16].

Moreover, the multipole kicker injection scheme was successfully implemented using MAX IV [17] and Sirius. A pulsed multipole magnetic kicker provides a special nonlinear field to kick the injected beam into the transverse acceptance of the storage ring, while the stored beam passes through the center of the kicker with a small disturbance. Although it is still an off-axis injection scheme, the disturbance to the stored beam is smaller compared with former schemes using bump kickers. However, this scheme requires a relatively small space due to only one magnet is used.

Longitudinal on-axis injection using an ultrashort pulse kicker separates the injected beam and stores it in time. The pulse width of the kicker must be sufficiently short to place the injected bunch transversely on the axis without disturbing

*tanjianhao@zjlab.org.cn

the circulating bunches. The injected bunch could be merged into the main bucket through synchrotron radiation damping. The transverse kick was provided by a pulsed dipole kicker in swap-out injection and longitudinal on-axis injection schemes.

A specially designed radio frequency (RF) system can be used to create a bucket for on-axis injection. Transverse kicks rely on short-pulse kickers. Longitudinal merging of the injected and stored bunches was achieved using the RF system. A double-frequency RF system has been employed in previous studies [5] [12]. Buckets for injection were created by altering the two RF voltages. After the injection, the inverse process of voltage alteration caused the injected bunches to enter the main RF buckets. In [12], an adjustment to the phase of the RF was added; thus, the control of the bucket could be more flexible. This also has a smaller impact on the stored bunches. In [13], a triple-frequency RF system was used to form a main bucket that could accommodate injected and stored bunches. The RF parameters remained unchanged and did not require adjustments during the injection period. In [14], a multi-objective optimization method for longitudinal injection using a multi-frequency RF system was presented. Finding an adapted design for different conditions would be helpful.

The common purpose of these schemes is use of a kicker to realize a transverse injection. The requirements for kickers are stringent. The rise and fall times are expected to be as short as possible. The full pulse duration and rise time should usually be on the order of nanoseconds. In addition to fast kicker magnets and pulsed multipole magnet kickers, the transverse kick can be provided by the crab cavity, which has been widely applied in bunch length measurements, emittance exchanges, and crab collisions. Kim *et al.* proposed an on-axis injection scheme using two pulsed transverse deflecting cavities [18]. The first cavity is located in the straight section upstream of the injection region and has $n\pi$ phase advance. The location of the second cavity depends on the injection site and septum. The second cavity kicked the injected beam into a closed transverse orbit. The stored beam passes through the two cavities, which offsets the interference to a certain extent and generates a disturbance in the emittance. They also investigated the effect of RF errors on emittance. A scheme based on a crab cavity is a solid foundation for research. Many studies on crab cavities have been conducted at the Shanghai Synchrotron Radiation Facility (SSRF) [19]. Injection of carb cavities is less technologically difficult.

In this paper, we propose a new longitudinal injection scheme inspired by the idea in [18] and based on experience in designing a crab cavity. A new type of crab cavity was produced and used to provide a transverse kick to inject the beam into a closed orbit in the horizontal plane. Two tubes were placed in each cavity: One is in an area without electromagnetic fields; thus, the stored beam usually runs undisturbed. The stored beam passes through two cavities in opposite fields, such that the total momentum deviation is zero. However, the two opposite transverse kicks have a betatron phase difference, which disturbs the emittance. The motion of the stored and injected beams was simulated. The effects of the bump orbit and wake field are discussed herein.

2. Scheme design of longitudinal injection

We used a cavity design different from that in [18]. The RF power was planned to be in the standing-wave mode rather than the pulse mode. This is because it is easier to maintain the amplitude and phase of the field repeating in the standing-wave mode. Two tubes were designed to satisfy the need for switching between the injection orbit and closed orbit in the crab cavity. The stored bunches passed through tube B at the usual times. When injection occurred, the stored bunches were kicked into tube A. Tubes A and B were connected using a slit for beam injection. The width of the slit should be close to the cutoff distance of the RF field in the cavity. A schematic of the injection process is displayed in Fig. 1 (a). Both cavities are located in a long straight section. The distance between them was shorter, and the disturbance of the stored beam was smaller than that in [18].

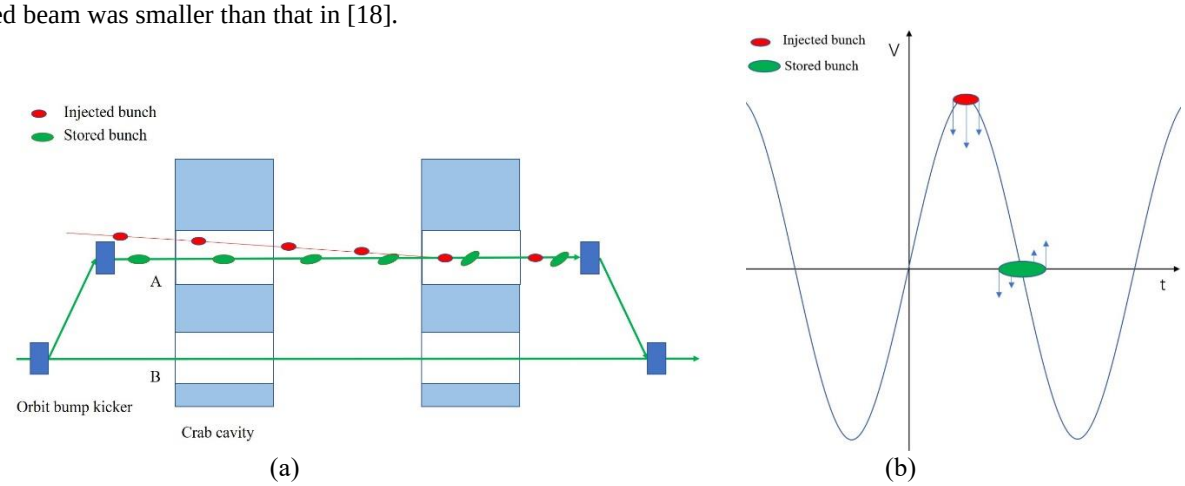

(a) (b)

Figure 1: Schematics of design: (a) Injection process; (b) Phases that injected bunches and stored bunches see in the first cavity.

The stored beam passed through tube B, where the electromagnetic (EM) field of the crab cavity was absent. The stored beam was kicked onto tube A by kickers, forming a closed bump orbit when the injection occurred. The two cavities are placed in tandem. When injected and stored bunches enter the two cavities, they will see different EM fields whose phase difference is π. When the stored bunch passed through the two cavities, the EM field phases were zero for the reference particles. Therefore, the reference particles were not affected by the crab cavity. The particles in the stored bunch, apart from the reference particles, are deflected or accelerated according to the EM field of the crab cavity, as shown in Fig. 1 (b). The phases that the injected bunch sees are π/2 and -π/2. Thus, they obtained the largest deflection force offered by the cavity. After passing through the first cavity, the injected bunch is deflected to the stored bunch. Their horizontal momentum was canceled after passing through the second cavity. Subsequently, the injected bunch entered the orbit of the stored bunch in the horizontal plane. The bump kickers kick them back into normal orbit. Finally, the injected bunch is merged into the stored bunch owing to synchrotron radiation damping.

The beams are mainly affected by the longitudinal and transverse magnetic fields in the cavity. According to the Panofsky–Wenzel theorem [20], the action of a cavity on the horizontal and longitudinal particles can be written as:

$$\Delta x' = \frac{eV}{E} sin(kz) \tag{1}$$

$$\Delta\delta = \frac{eVkx}{E}\cos(kz) \tag{2}$$

$$k = \frac{2\pi f}{c} \tag{3}$$

where $\Delta x'$ is the relative horizontal momentum change of the particle, $\Delta\delta$ is the relative energy change of the particle, V is the deflection voltage, E is the particle energy, z is the longitudinal coordinate of the particle, x is the horizontal coordinate of the particle, c is the velocity of light, and f is the work frequency of the cavity.

The particles in the stored bunch had different horizontal momenta because of their various longitudinal coordinates after passing through the first cavity. They exhibited a horizontal displacement before reaching the second cavity. The particles act opposingly in the second cavity, which cancels out their horizontal momentum. The transfer matrix of the crab cavity can be written as follows:

$$\begin{pmatrix} x \\ x' \\ y \\ y' \\ z \\ \delta \end{pmatrix} = \begin{bmatrix} 1 & 0 & 0 & 0 & 0 & 0 \\ 0 & 1 & 0 & 0 & u & 0 \\ 0 & 0 & 1 & 0 & 0 & 0 \\ 0 & 0 & 0 & 1 & 0 & 0 \\ 0 & 0 & 0 & 0 & 1 & 0 \\ u & 0 & 0 & 0 & 0 & 1 \end{bmatrix} \begin{pmatrix} x_0 \\ x'_0 \\ y_0 \\ y'_0 \\ z_0 \\ \delta_0 \end{pmatrix}$$

$$u = \frac{keV}{E} \tag{4}$$

The transfer matrix of the whole structure can be expressed as:

$$\begin{pmatrix} x \\ x' \\ y \\ y' \\ z \\ \delta \end{pmatrix} = \begin{bmatrix} 1 & L & 0 & 0 & uL & 0 \\ 0 & 1 & 0 & 0 & 0 & 0 \\ 0 & 0 & 1 & L & 0 & 0 \\ 0 & 0 & 0 & 1 & 0 & 0 \\ 0 & 0 & 0 & 0 & 1 & 0 \\ 0 & -uL & 0 & 0 & -u^2L & 1 \end{bmatrix} \begin{pmatrix} x_0 \\ x'_0 \\ y_0 \\ y'_0 \\ z_0 \\ \delta_0 \end{pmatrix}$$

where L denotes the distance between the two cavities. The geometric relationship between these variables can be written as:

$$\frac{d}{L} = \frac{eV}{E} \tag{5}$$

$$x'_0 + \frac{eV_1}{E} = \frac{eV}{E} \tag{6}$$

$$\Delta x = \Delta x' L \tag{7}$$

where d is the horizontal distance between the injected beam and the bump orbit at the beginning of injection, x'_0 is the initial relative horizontal momentum, V_1 is the deflection voltage that the injected bunches received in the first cavity, and Δx is the horizontal displacement of the particles. Combining Equations (1), (3), (5), and (7), the horizontal displacement equals the product of d and $\sin(kz)$. Consequently, the disturbance to the stored beam depends on the transverse offset of the injection beam at the septum, frequency of the cavity, and bunch length. This is independent of the injection direction (horizontal or vertical). The injection direction depended on the dynamic aperture. For the lattice used, the dynamic aperture in the horizontal direction is larger. Therefore, the beams were injected horizontally.

3. Beam dynamic simulation of longitudinal injection based on C-band crab cavity

A C-band standing-wave crab cavity was preliminarily designed. The operating frequency was set to 5500 MHz. The height of the bump orbit, i.e., the distance between the centers of the two tubes, was set to 45 mm. It comprises five regularities. A cut-view model of a 5-cell crab cavity is depicted in Fig. 2. A racetrack-shaped structure was selected to cancel the polarization degeneracy mode [19].

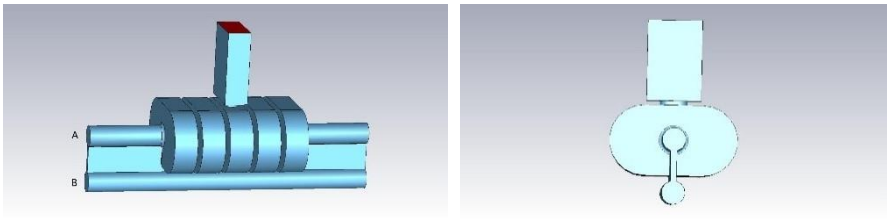

(a) (b)

Figure 2: Cut view model of 5-cell crab cavity: (a) Simulated pattern; (b) Left view.

Accelerator Toolbox version 2.0 was employed for simulation [21]. The lattice used for the simulation was a five-bend achromat lattice, the main parameters of which are summarized in Table 1. It has four long straight sections, one of which was used for injection. The positions of these components are shown in Fig. 3. The injected beam entered the first cavity at the angle of 0.143 mrad and 5 mm above the center of tube A. The deflection voltage at the center of tube A was 4 MV. The main consideration of this design was to ensure that the injection beam was in the center of the second cavity. Two thousand macroparticles with a Gaussian distribution in a six-dimensional phase space were considered to simulate the bunches. The simulation only provides a principle verification of the scheme and does not consider machine and injection errors.

Table 1: The Main Lattice Parameters

Parameter	Value	Unit
Energy	0.8	GeV
Circumference	168	m
Natural Energy Spread	0.00049	
Horizontal Emittance	0.885	nm-rad
Vertical Emittance	0.000686	nm-rad
Linear Energy Acceptance	4.18%	
RMS Bunch Length	1.46	mm
Damping Time (x,y,z)	42.96,50.23,27.43	ms
Dynamic Aperture (x,y)	12,5	cm
RF Frequency	499.65	MHz
RF Voltage	606	kV

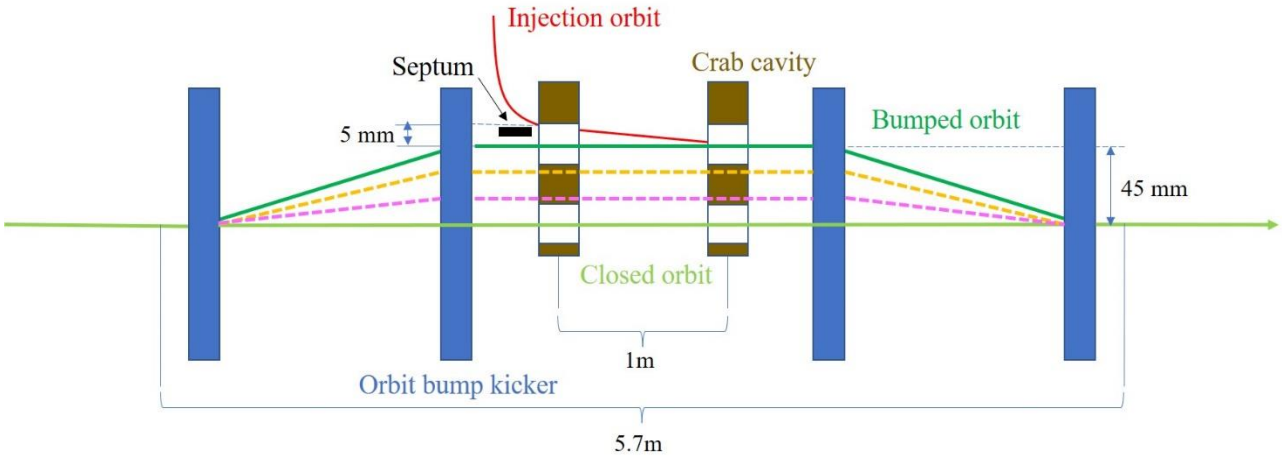

Figure 3: Crab cavity injection scheme layout

Figure 4 (a) presents the distortion of the stored bunch in the horizontal phase space when injection occurs. The deep red dots denote the initial stored bunch, and the blue dots show the bunch after passing through the injection system. The five strips on the left depict the first five turns of the storage ring. The maximum horizontal displacement of particles in the stored bunch was approximately 3 mm. Figure 4 (b) shows that the horizontal emittance of the stored beam increased sharply after injection and returned to the normal level after approximately 170,000 turns. Figure 4 (c) shows the change in the injected bunch after passing through the two cavities in the horizontal phase space. The blue dots denote the injected bunch at the beginning of injection. The injected bunch was placed exactly at the center of the horizontal plane, and its horizontal displacement was smaller than that of the stored bunch. This is mainly because the length of the injected bunch is 0.2 mm, which is much shorter than that of the stored bunch, and the field to the injected bunch is the peak of the wave, where the slope is the smallest. Thus, the forces on the different particles are close. Figure 4 (d) shows that the injected bunches were longitudinally accepted from the start and damped at the center of the bucket. This is because the injected bunch was just 0.25 of the wavelength of the cavity behind the stored bunch. The tune frequency of the lattice was one eleventh of the cavity work frequency. Thus, the momentum acceptance was sufficient.

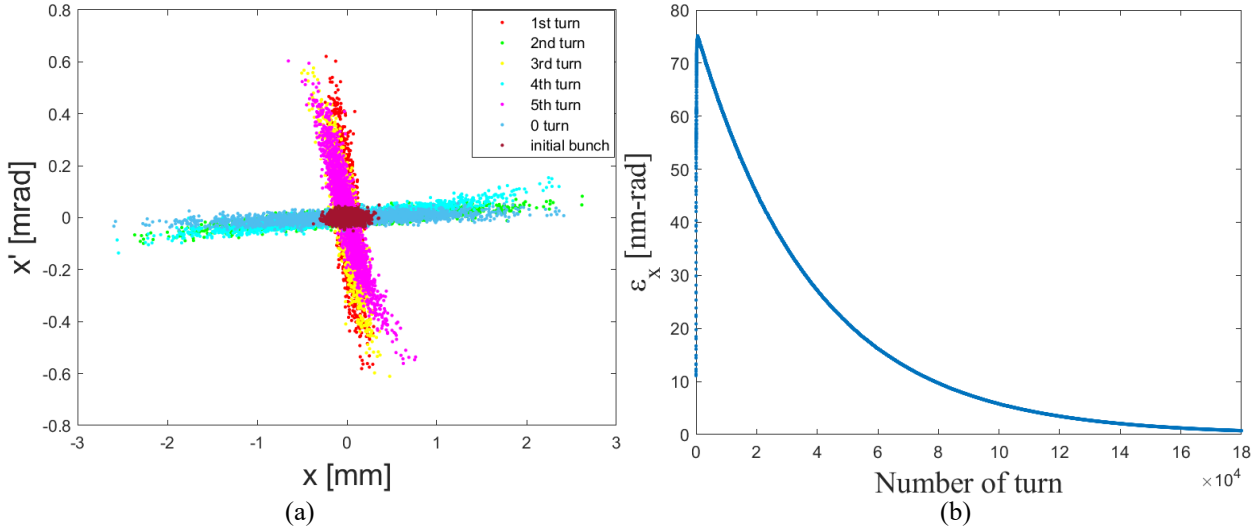

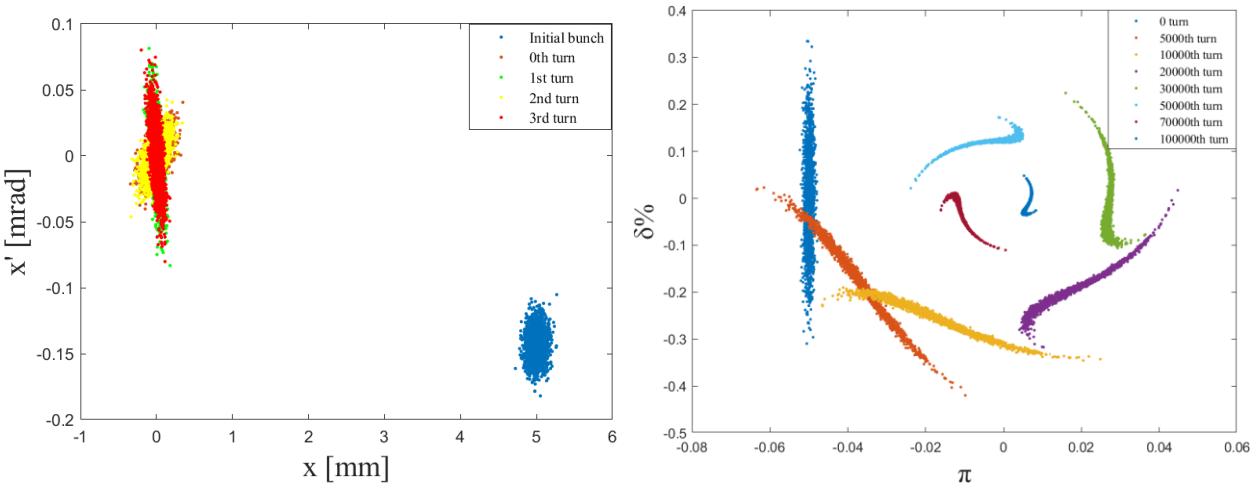

(c) (d)

Figure 4: Influence to stored bunch: (a) Stored bunch in horizontal phase space; (b) Change in horizontal emittance with number of turns; (c) Injected bunch in horizontal phase space; (d) Damping of injected bunch in longitudinal phase space.

4. Discussion

4.1 Multiple bunch injection

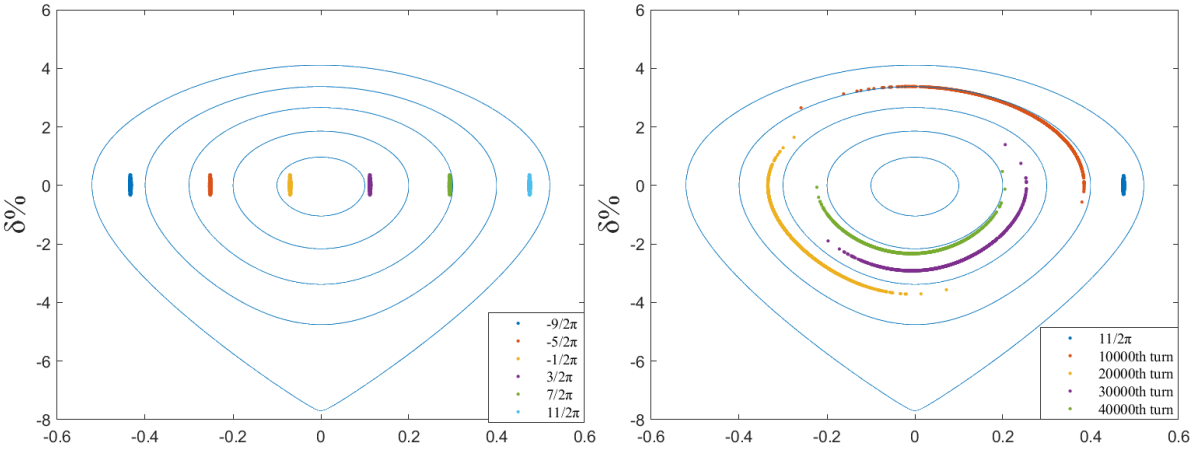

(a) (b)

Figure 5: Injected bunches in bucket: (a) A bucket can hold up to six injected bunches; (b) Damping of bunch injected in phase of 11/2π.

The frequency of the cavity is significantly higher than that of the RF cavity. Therefore, a bucket can hold more than one bunch, whose phase difference is 2π. Figure 5 (a) presents the six injected bunches in different phases. Figure 5 (b) depicts the motion of the bunch in 11/2π, which is the farthest bunch that can be held. This implies that up to six bunches could be injected simultaneously; all of them damped to the center of the bucket.

4.2 Extra quantum excitation

The difference in length between the normal and bump orbits was approximately 1.35 mm. This slight deviation caused a small oscillation. The synchrotron oscillation period was 0.217 ms (388 turns). An increase in the orbit length will result in a slight extra quantum excitation. The increment in the horizontal direction can be calculated as:

$$\frac{\sigma_x^2}{\beta_x} = \frac{J_z}{J_x}\frac{\eta^2}{\beta_x}\delta^2 \tag{8}$$

$$\sigma_l^2 = \frac{l}{C}\sigma_x^2 \tag{9}$$

where σ_x^2 is the rms value of horizontal displacement caused by quantum excitation, σ_l^2 is the part caused by bump orbit, J_z and J_x are the damping partition numbers, η is the dispersion function, δ is energy spread, β_x is the beta

function, l is the increment of orbit, and C is the circumference of the storage ring. The increased σ_x is 3.73 pm, which is small compared with the rms value of the stored bunch [22].

4.3 Influence of bump and phase error

The stored beam passes through the area without an electromagnetic field and that with a smaller field strength successively during the process of bump orbit generation, and finally reaches the center of tube A, where the field strength is the largest. For example, the dotted purple line in Fig. 3 denotes a stored beam lifted by 15 mm. The difference in length between this orbit and the normal orbit was approximately 0.15 mm. The orange dotted line represents the stored beam lifted by 30 mm. The corresponding deflection voltage was 3.66 MeV. The difference in length between this orbit and the normal orbit was approximately 0.6 mm. The variation trend of the horizontal emittance is presented in Fig. 4 (b). Therefore, the maximum horizontal emittance was selected as the characteristic indicator. Figure 6 (a) shows that the cavity field has a significant impact on the stored beam emittance, which is positively correlated with the bump height.

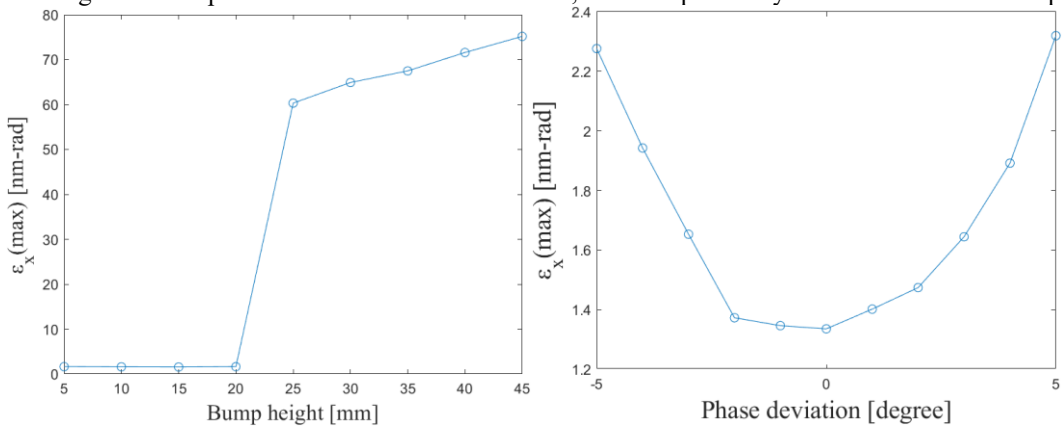

Figure 6: Change in maximum horizontal emittances of (a) stored beam with bump height, and (b) injected beam with phase deviation of the second cavity.

The working frequency of the cavity must be a multiple of the tuning frequency of the storage ring. According to the simulation results, the bump orbit of 45 mm is acceptable. The straight section used for the injection was limited, and the size of the cavity was related to the work frequency. Therefore, it is necessary to balance these two parameters. The stability of the cavity field amplitude should also be considered. Suppose the amplitude fluctuates +/-0.04%. Thus, the stored bunches are most affected when they are 1.0004 times the set value in the first cavity and 0.9996 times the set value in the second cavity. In this case, the maximum horizontal emittance was 75.32 nm-rad. This increment is small compared with the situation in which the amplitude is precise (75.17 nm-rad). Considering the phase error, the influence of the injected beam was significantly greater than that of the stored beam. The phase deviation of the second cavity was simulated from -5° to +5° assuming the phase of the first cavity is accurate. The phase deviation causes an increase in the horizontal emittance, as shown in Fig. 6 (b). This growth rate was exponential. Therefore, it is important to ensure the phase accuracy.

4.4. Long-range wake field of the crab cavity

The cavity structure is not symmetric. Therefore, the wake field induced by the stored beam should be considered. The filling percentage was set to 70% and the current intensity was set to 1 A. In this case, 196 stored bunches were present in the storage ring. The charge of each stored bunch was 2.8591 nm. Figures 7 (a)–(c) provide the simulation results of the wake potential induced by one stored bunch 1 mm from the center in the first 200 m. The wake field to a stored bunch equals the superposition of the wake fields induced by the foregoing bunches, including itself, in the previous turns. Moreover, Figs. 7 (a)–(c) show that the wake field decayed exponentially with time. Therefore, the wake field to the stored bunches reaches a maximum and stops increasing after a few turns. For calculation convenience, the data from the first three turns (i.e., 504 m) were adopted. The corresponding simulation results are displayed in Figs. 7 (d), (e): the blue line represents the case that does not consider the wake field, while the red line represents the case in which the wake field is considered. The two lines almost overlap in Figs. 7 (d) and (e). This demonstrates that the long-range wake field has little effect on the stored beams. Further, the wake field has less of an effect on the injected beam because the charge of the injected bunch is smaller than that of the stored bunch.

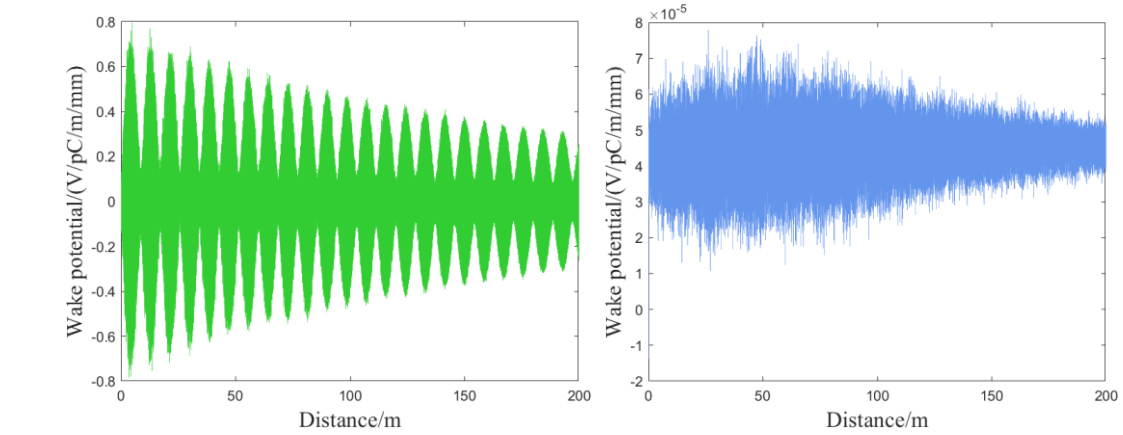

(a) (b)

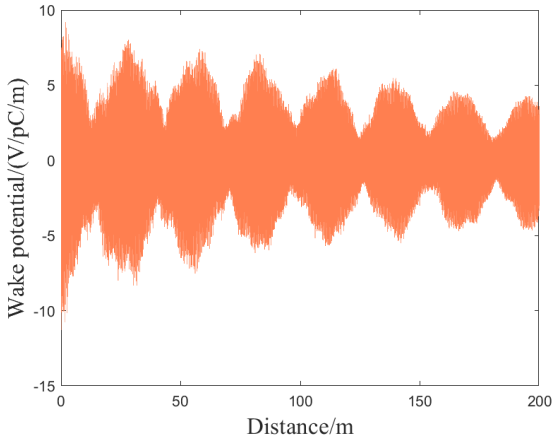

(c)

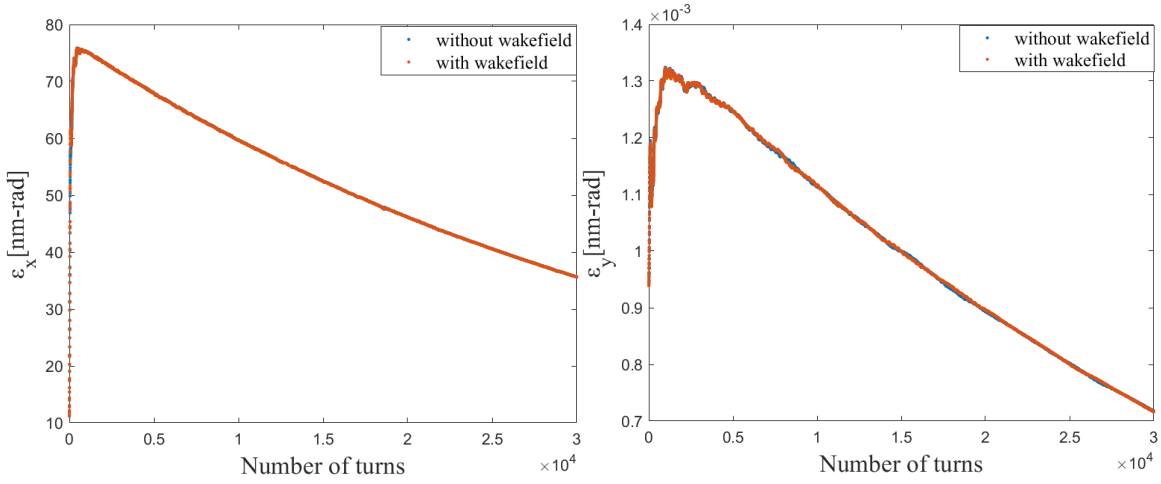

(d) (e)

Figure 7: Wake potential in (a) horizontal, (b) vertical, and (c) longitudinal; and change in (d) horizontal and (e) vertical emittance.

5. Implementation of crab cavity and cold test results

A five-cell crab cavity was produced according to the design scheme and development process of the crab cavity [23]. The cavity comprises a conventional standing-wave crab cavity and an additional tube (tube B). The deflecting cavity

was connected to tube B using a slit with the width of 4 mm. The electromagnetic field from the crab cavity cannot be transferred into tube B because the slit cuts it off. The primary dimensions of the cavity are listed in Table. 2. As can be seen, the established crab cavity can provide the deflecting voltage of 4 MV and input power of 2 MW.

Table 2: The Main Parameters of the Cavity

Parameter	**Value**	**Unit**
Operation Frequency	5500	MHz
Operation Mode	Pi	/
Tube Aperture	20	mm
Single Cavity Length	27.25	mm
Disc Thickness	5	mm
Distance between Two Tubes	45	mm
Vacuum Plate Spacing	5	mm
Transverse Shut Impedance R	1.65	MΩ
Quality Factor Q	14133	/
R/Q	116.5	Ω
Cell Number	5	/
Input Power	2	MW
Transverse deflecting Voltage	4	MV

Mechanical design drawings of a single cell and the total structure are displayed in Figs. 8 (a) and (b), respectively. Each cell includes eight holes of 8 mm each for cooling water flow. A resonant perturbation method and the “cage” type perturbing object were used on the transverse electric field measurement and tune when fabrication and brazing of the cavity were finished [24-26]. The “cage” type perturbing object was adopted to measure the electric field in the direction of polarization, but the effect of longitudinal electric field cannot be eliminated completely [27]. A crab cavity prototype is depicted in Fig. 8 (c).

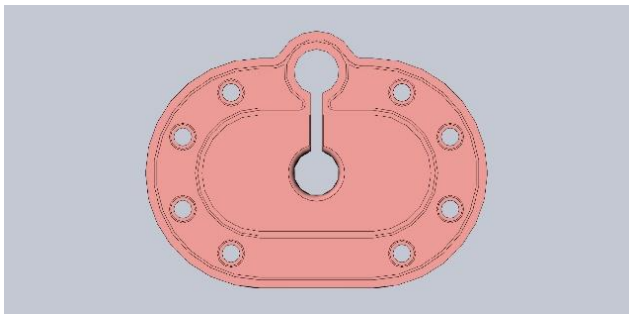

(a)

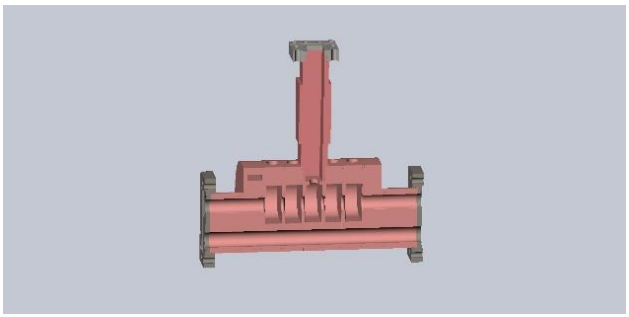

(b)

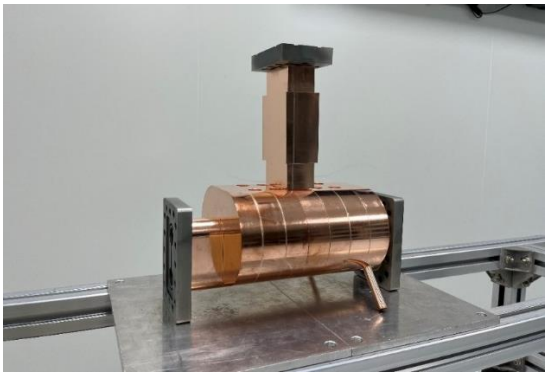

(c)

Figure 8: Structure of crab cavity: (a) Pattern of cell; (b) Pattern of crab cavity; (c) Prototype of crab cavity.

The simulated and measured results for the transverse electric field are shown in Fig. 9. The measurement result of the field distribution was the combined transverse and longitudinal fields, which is almost the same as the simulation result.

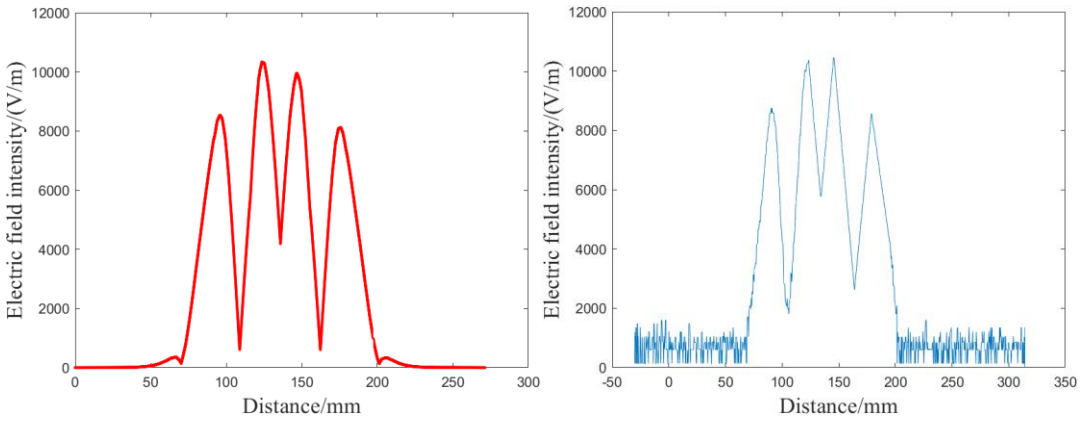

(a) (b)

Figure 9: Electric field distribution: (a) Simulation result; (b) Measurement result.

6. Conclusion

A longitudinal injection scheme based on a new type of crab cavity is proposed in this paper. Two C-band crab cavities were considered to complete the longitudinal injection without a short-pulse kicker, switching the temporal challenge to a spatial issue. The simulation results show almost no horizontal centroid oscillation in the injection beam. The horizontal disturbance of the head and tail particles of the stored bunches was approximately 3 mm. Thus, the dynamic aperture should be greater than 3 mm. This requirement can be reduced by lowering the crab cavity frequency. However, it increases the size of the cavity and the orbit bump amplitude. In addition, the disturbance to the stored beam during the bump orbit generation process was investigated. The long-range wake field induced by the stored beam was simulated and its effect on emittance was found to be small. A crab cavity was successfully created, providing the basis for realizing the scheme. The field distributions of the cavities were also measured. All the parameters of the cavity meet the requirements. The field distribution measurement results are consistent with the simulation results. As a result, the proposed scheme has improved error reduction in the cavity and upgrade of the septum. The phase error reduction of the cavity is critical for the scheme to perform. Further, improving the septum to decrease the transverse offset of the injection beam can directly reduce disturbance to the stored beam.

Funding

This study was supported by the National Natural Science Foundation of China (Grant Numbers 11975298 and 12175292).

References

[1] Y. Zhao, Y. Jiao, S. Wang, Design study of APS-U-Type hybrid-MBA lattice for mid-energy DLSR. Nucl. Sci. Tech. 32, 71 (2021). doi:10.1007/s41365-021-00902-1

[2] P.H. Yang, W. Li, Z.L. Ren et al., Design of a diffraction-limited storage ring lattice using longitudinal gradient bends and reverse bends. Nucl. Instrum. Meth A. 990, 164968 (2021). doi:10.1016/j.nima.2020.164968

[3] S. C. Leemann, A. Andersson, M. Eriksson et al., Beam dynamics and expected performance of Sweden's new storage-ring light source: MAX IV. Phys. Rev. Accel. Beams. 12, 120701 (2009). doi:10.1103/PhysRevSTAB.12.120701

[4] Y. Cai, K. Bane, R. Hettel et al., Ultimate storage ring based on fourth-order geometric achromats. Phys. Rev. Accel. Beams. 15, 054002 (2012). doi:10.1103/PhysRevSTAB.15.054002

[5] B.C. Jiang, Z.T. Zhao, S.Q. Tian et al., Using a double-frequency RF system to facilitate on-axis beam accumulation in a storage ring. Nucl. Instrum. Meth A. 814 (2016). doi:10.1016/j.nima.2016.01.024

[6] P. Raimondi, N. Carmignani, L. R. Carver et al., Commissioning of the hybrid multibend achromat lattice at the European Synchrotron Radiation Facility. Phys. Rev. Accel. Beams. 24,110701(2021). doi:10.1103/PhysRevAccelBeams.24.110701

[7] Spring-8-II conceptual design report, http://rsc.riken.jp/eng/index.html.

[8] J. Bengtsson and A. Streun, Report No. SLS2-BJ84-001, 2017.

[9] C. Steier, A. Anders, S. De Santis et al., On-Axis Swap-Out Injection R+D for ALS-U, in Proc. IPAC'17, Copenhagen, Denmark, May 2017, pp. 2821-2823. doi:10.18429/JACoW-IPAC2017-WEPAB103

[10] S. C. Leemann, Pulsed sextupole injection for Sweden's new light source MAX IV. Phys. Rev. Accel. Beams. 15, 050705 (2012). doi:10.1103/PhysRevSTAB.15.050705

[11] M. Aiba, M. Böge, F. Marcellini et al., Longitudinal injection scheme using short pulse kicker for small aperture electron storage 4rings. Phys. Rev. Accel. Beams. 18, 020701 (2015). doi:10.1103/PhysRevSTAB.18.020701

[12] G. Xu, J. H. Chen, Z. Duan et al., On-axis Beam Accumulation Enabled by Phase Adjustment of a Double-frequency RF System for Diffraction-limited Storage Rings, in Proc. IPAC'16, Busan, Korea, May 8-13 2016 pp. 2032-2035. doi:10.18429/JACoW-IPAC2016-WEOAA02

[13] S. C. Jiang, G. Xu, On-axis injection scheme based on a triple-frequency rf system for diffraction-limited storage rings. Phys. Rev. Accel. Beams. 21, 110701 (2018). doi:10.1103/PhysRevAccelBeams.21.110701

[14] W.H. Liu, Y. Jiao, Y. Zhao et al., Multi-objective optimization of longitudinal injection based on a multi-frequency RF system for fourth-generation storage ring-based light sources. Nucl. Instrum. Meth A. 1046, 167712 (2023) doi:10.1016/j.nima.2022.167712

[15] Advanced photon source upgrade project, Final design report, Argonne National Laboratory Technical Report No. APSU-2.01-RPT-003, 2019.

[16] Y. Jiao, G. Xu, X.H. Cui et al., The HEPS project. J. Synchrotron Rad. 25, 1611 (2018). doi:10.1107/S1600577518012110

[17] P. Alexandre, R.B. Fekih, A. Letrésor et al., Transparent top-up injection into a fourth-generation storage ring. Nucl. Instrum. Meth A. 986, 164739 (2021). doi:10.1016/j.nima.2020.164739

[18] J. Kim, G. Jang, M. Yoon et al., Phys. Rev. Accel. Beams. 22, 011601 (2019). doi:10.1103/PhysRevAccelBeams.22.011601

[19] J. H. Tan, Q. Gu, W. C. Fang et. al. X-band deflecting cavity design for ultra-short bunch length measurement of SXFEL at SINAP, Nucl. Sci. Tech. 25, 060101 (2014). doi:10.13538/j.1001-8042/nst.25.060101

[20] W.K.H. Panofsky, W. A. Wenzel, Some considerations concerning the transverse deflection of charged particles in radio-frequency fields. Rev. Sci. Instrum. 27, 967 (1956). doi:10.1063/1.1715427

[21] Accelerator Toolbox version 2.0. https ://github.com/atcollab/at

[22] Z.P. Liu, Introduction to the physics of synchrotron radiation light sources (Hefei, 2009)

[23] J. H. Tan, W.C. Fang, D.C. Tong et al., Design, RF measurement, tuning and high-power test of an X-band deflector for Soft X-ray Free Electron Lasers (SXFEL) at SINAP. Nucl. Instrum. Meth A. 930,21 (2019). doi:10.1016/j.nima.2019.03.093

[24] D. Tong, A new type of perturbing object for high order mode measurements in resonant cavities. DESY M-87-06 (1987)

[25] L. Xiao, Y. Liang, D. Tong et al., Measurements of higher order modes in a 30 cm long X-band structure. Nucl. Instrum. Meth A. 463, 1-2 (2001). doi:10.1016/S0168-9002(01)00468-5

[26] J. C. Amato and H. Herrmann, Improved method for measuring the electric field in microwave cavity resonators. Rev. Sci. Instrum. 56, 696 (1985). doi:10.1063/1.1138208

[27] J. H. Tan, D.C. Tong, Q. Gu et al. Development of a nonresonant perturbation technique and its application to multicell traveling-wave deflectors. Nucl. Instrum. Meth A. 835,1 (2016). doi:10.1016/j.nima.2016.08.039